

Pentapeptide modified ethosomes for enhanced skin retention and topical efficacy activity of indomethacin

Jiangxiu Niu^{a*}, Ming Yuan^{a*}, Hongying Li^b, Yao Liu^a, Liye Wang^a, Yanli Fan^a, Yansong Zhang^a, Xianghui Liu^a, Lingmei Li^a, Jingxiao Zhang^a and Chenyu Zhao^a

^aCollege of Food and Drug, Henan Functional Cosmetics Engineering & Technology Research Center, Luoyang Normal University, Luoyang, Henan, China; ^bDepartment of Pharmacy, Affiliated Hospital of Weifang Medical University, Weifang, China

ABSTRACT

Challenges associated with topical analgesics and anti-inflammatory drugs include poor drug penetration and retention at the desired lesion site. Therefore, improving these challenges would help to reduce the toxic and side effects caused by drug absorption into the systemic circulation and improve the therapeutic efficacy of topical therapeutic drugs. Pentapeptide (KTTKS) is a signal peptide in skin tissue, it can be recognized and bound by signal recognition particles. In the current study, we successfully prepared novel indomethacin (IMC) loaded KTTKS-modified ethosomes (IMC-KTTKS-Es), and the physicochemical properties and topical efficacy were investigated. Results showed that the prepared IMC-KTTKS-Es displayed a particle size of about 244 nm, a negative charge, good deformability, and encapsulation efficiency (EE) exceeding 80% for IMC, with a sustained release pattern. In vitro percutaneous permeation studies revealed that the skin retention was increased after the drug was loaded in the IMC-KTTKS-Es. Confocal laser scanning microscopy also showed improved skin retention of IMC-KTTKS-Es. In addition, IMC-KTTKS-Es showed improved topical analgesic and anti-inflammatory activity with no potentially hazardous skin irritation. This study suggested that the IMC-KTTKS-Es might be an effective drug carrier for topical skin therapy with a good safety profile.

ARTICLE HISTORY

Received 22 March 2022
Revised 10 May 2022
Accepted 16 May 2022

KEYWORDS

Pentapeptide; indomethacin; ethosomes; skin permeation and retention; efficacy activity

1. Introduction






Indomethacin (IMC) is a widely used non-steroidal anti-inflammatory drug (NSAIDs) with potent topical analgesic and anti-inflammatory pharmacological effects (Nagai et al., 2019). It can also be used to treat topical skin diseases, such as localized pain and inflammation, solar dermatitis, herpes, erythema nodosum, hair folliculitis, etc (Froelich et al., 2017). IMC is marketed in oral dosage forms in many countries, with a few marketed as parenteral and topical dosage forms. However, oral IMC is difficult to achieve effective therapeutic concentration topically, and has strong adverse reactions of gastrointestinal irritation and bleeding, which limits its wide clinical application (Toropainen et al., 2021). One well-known method to avoid these side effects-related problems is transdermal topical administration.

Compared with oral administration and other routes of administration, transdermal topical administration could reduce gastrointestinal side effects and the number of drugs entering the blood circulation, thereby reducing systemic adverse effects. Therefore, the transdermal route is one of the ways to overcome the problems of oral NSAIDs (El Maghraby, 2010). However, the stratum corneum (SC) limits

the number of drugs entering the active epidermis and dermis, resulting in drug waste and poor clinical efficacy after topical administration (Kapoor et al., 2017). Studies have shown that the preparation of drugs in appropriate dosage forms for topical administration can effectively increase topical absorption and retention of drugs, thereby increasing the topical efficacy activity (Aragao Horoiwa et al., 2020).

Traditional liposomes could promote the transdermal absorption of drugs (Doppalapudi et al., 2017). However, due to the large size and lack of elasticity, most of the traditional liposomes are limited to the upper layer of the SC and have limited penetration into the deep tissue (Abd et al., 2021). Ethosomes could penetrate the SC into the deep layer of the skin, and its percutaneous permeability is demonstrated to be superior to that of traditional liposomes (Zhang et al., 2014). However, common nanocarriers for topical administration, including ethosomes, cannot effectively stay in the skin when treating tropical diseases. Therefore, for the drugs used for local treatment, it is necessary to further enhance the retention effect of the drug in the skin, so as to further enhance the local treatment effect.

Lysine-threonine-threonine-lysine-serine is a short peptide derived from collagen hydrolysis and its more stable form is

CONTACT: Hongying Li  hongying8624@126.com  Department of Pharmacy, Affiliated Hospital of Weifang Medical University, Weifang, 261031, China; Liye Wang  liye2009314@163.com; Yanli fan  fanyanli06@163.com  College of Food and Drug, Henan Functional Cosmetics Engineering & Technology Research Center, Luoyang Normal University, Luoyang, Henan, 471934, China

*Authors of Jiangxiu Niu and Ming Yuan contributed equally to this work.

© 2022 The Author(s). Published by Informa UK Limited, trading as Taylor & Francis Group.

This is an Open Access article distributed under the terms of the Creative Commons Attribution-NonCommercial License (<http://creativecommons.org/licenses/by-nc/4.0/>), which permits unrestricted non-commercial use, distribution, and reproduction in any medium, provided the original work is properly cited.

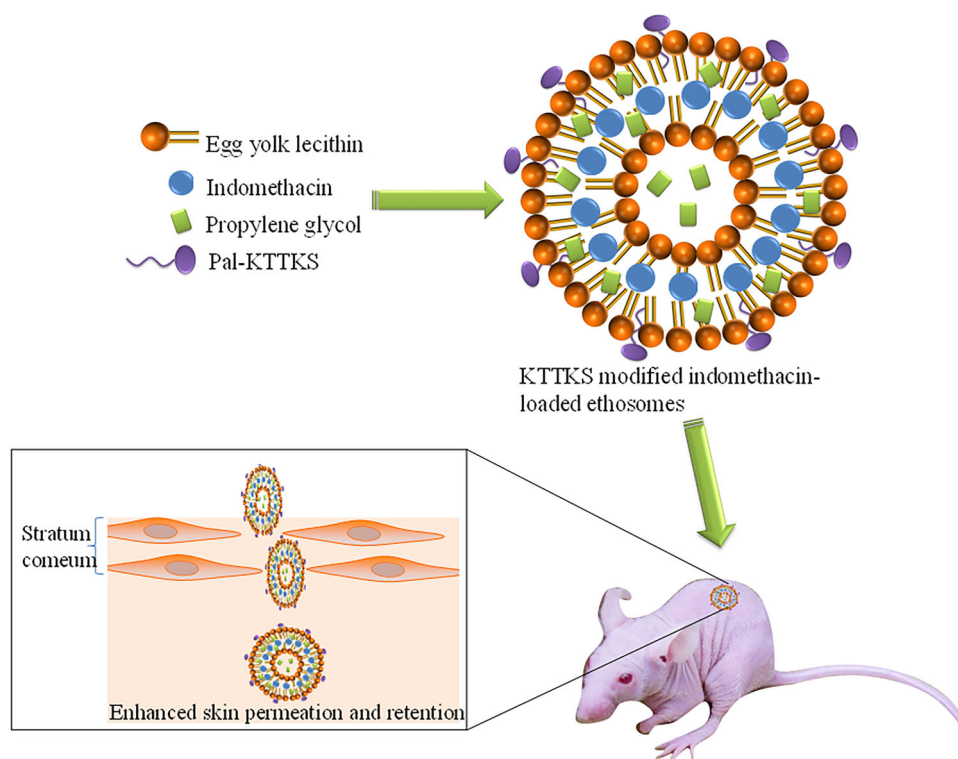


Figure 1. Schematic illustration of the preparation of IMC-KTTKS-Es for enhanced skin permeation and retention.

palmitoyl-pentapeptide (Pal-KTTKS), which is a derivative of KTTKS combined with palmitoyl. It is easy to penetrate the SC of the skin due to its good interaction with the skin. KTTKS is a signal peptide in skin tissue, it can be recognized and bound by signal recognition particles (SRP) in skin tissues, and promote the synthesis of matrix proteins, especially collagen, by increasing the activity of stromal cells (Tałaaj et al., 2019). Signal peptides can be used to modify nano drug delivery systems to improve the functionality of preparations (Bae et al., 2021). In light of this, KTTKS might be used in nano-drug delivery systems to improve the intradermal retention of the drug in the lesion site through the interaction between KTTKS and proteins in the skin, thus enhancing the therapeutic effect.

Therefore, the aim of this study was to develop IMC-loaded KTTKS-modified ethosomes (IMC-KTTKS-Es) for enhanced skin retention and topical efficacy activity of IMC (Figure 1). For this purpose, IMC-KTTKS-Es were prepared by the conventional thin-film evaporation and hydration method. The developed nanosystem was characterized by particle size distribution, polydispersity index (PDI), zeta potential, surface morphology, encapsulation efficiency (EE), deformability, X-ray diffraction (XRD), Fourier Transformed Infrared spectroscopy (FTIR) and *in vitro* release. Further *in vitro* percutaneous permeation was carried out using Franz diffusion cells and the effect of the formulation on skin microstructure was studied by the hematoxylin and eosin (HE) staining method. Furthermore, confocal laser scanning microscopy (CLSM) was used to visualize the skin delivery and penetration of drugs in porcine ear skin. Besides, the *in vivo* anti-inflammatory and analgesic activity was evaluated in mice.

2. Materials and methods

2.1. Materials

Indomethacin (IMC) was provided by Shanxi HaoChen Biotechnology Co., Ltd (China); Egg yolk lecithin (EYL) was purchased from Nanjing Dulai Biotechnology Co., Ltd (China); Palmitoyl pentapeptide (Pal-KTTKS) was supplied by Chongqing Gaide Chemical Co., Ltd (China). Carbopol-940 was provided by BASF Corporation (Germany). Coumarin-6 was supplied by Hefei Bomei Biotechnology Co., Ltd (China). Xylene was obtained from Shanghai Aladdin Reagent Co., Ltd (China). Other reagents were analytical grade preparation.

2.2. Animals

ICR mice (male, 18–22 g weight) were purchased from the Henan Experimental Animal Center, Zhengzhou, China. All animals were housed in a constant temperature and humidity room with a 12 h light cycle and had free access to food and tap water before the experiments. The experimental protocols were in accordance with the guidelines approved by Luoyang Normal University, and the study was approved by the Institutional Animal Ethics Committee.

2.3. Preparation and optimization of IMC-KTTKS-Es

IMC-KTTKS-Es were prepared using the conventional thin-film evaporation and hydration method. Briefly, egg yolk lecithin (0.3 g), IMC (0.1 g) and Pal-KTTKS (5, 10, 20, 40, and 60 mg of Pal-KTTKS were added separately to optimize the best amount in the formulation) were co-dissolved in 10 mL

anhydrous alcohol and mixed for 5 min in a flask. Subsequently, the organic solvent was removed thoroughly from the mixture at reduced pressure and 50 °C to form a thin lipid film. Then, the dried, lipid film was hydrated with 20 mL of 15% propylene glycol aqueous at 50 °C. Finally, the dispersions were ultrasonicated (KQ-250DE, Kunshan Ultrasonic Instrument Co., Ltd, Kunshan, China) for 5 min to achieve smaller-sized nanoparticles. The preparation method of IMC-loaded ethosomes without modified KTTKS (IMC-Es) was similar to that described above. The conducted formulation of IMC-KTTKS-Es was loaded in Carbopol® 940 gel (IMC-KTTKS-Es gels) to make it acceptable in consistency for topical skin application

2.4. Characteristics of the formulation

2.4.1. Particle size, zeta potential and surface morphology

The particle size, size distribution, polydispersity index (PDI) and zeta potential of the formulation was measured using the instrument Zetasizer Nano (Nanozs 90, Malvern Panalytical, UK). The surface morphology of IMC-KTTKS-Es was observed by field emission Scanning electron microscope (SEM) (Sigma 500, ZEISS, Germany).

2.4.2. Encapsulation efficiency (EE)

The entrapment efficiency (EE) values of the formulation were determined via an indirect method using ultracentrifugation (Wang et al., 2016; Vasanth et al., 2020). In brief, about 1.0 mL of the formulation was taken in an ultrafiltration centrifuge tube (MWCO: 30 kDa) and subjected to centrifugation at a speed of 5000 rpm for 10 min, the unencapsulated free drug from ethosome vesicle system was separated, and the supernatant layer was collected. The IMC in the supernatant was analyzed at 320 nm by UV-Vis spectrometry (TU-1810PC, Purkinje, Beijing, China), and the values of EE% were calculated according to the following equation:

$$EE\% = (IMC_{total} - IMC_{free}) / IMC_{total} \times 100\%$$

where IMC was initially added was considered as IMC_{total} and the amount of IMC in the supernatant was IMC_{free} .

2.4.3. Deformability measurement

The deformability of the IMC-KTTKS-Es formulations was measured by extrusion through a 150 nm filter membrane (Dudhipala et al., 2020). Briefly, suspension of IMC-KTTKS-Es was squeezed through a polycarbonate filter membrane with a pore diameter of 150 nm at 0.45 MPa for 5 min, the volume of vesicular suspension which was extruded during 5 min was measured. The deformability of the deformable ethosomes was calculated by using the following formula:

$$D = J_{flux} \times (r_v / r_p)^2$$

where D is the deformability of ethosomes; J is the volume of suspension which was extruded during 5 min; r_v is the size of ethosomes (after passing); and r_p is the pore size of the filter membrane.

2.4.4. In vitro release

In vitro, drug release studies were performed using a vertical glass Franz diffusion instrument (RYJ-6B, Shanghai Huanghai Drug Control Instrument Co., Ltd, China) at 37 °C. A dialysis membrane with a molecular weight cutoff value of 3500 Da was used to separate the compartments, the donor side with a release surface area of 2.8 cm² and the receptor side containing 6.5 mL of PBS buffer (pH = 7.4) as release medium. The release medium is stirred by a magnetic stirrer rotating at approximately 300 rpm. 0.5 g of IMC plain gel, IMC-Es gel and IMC-KTTKS-Es gel was respectively used in the donor compartment. All gel formulations contained 3% (w/w) IMC. 0.5 mL of the receptor medium were taken at predetermined intervals of 2, 4, 8, 12, 24, and 48 h, and the amount of the IMC in each sample was determined via a high-performance liquid chromatography (HPLC) system (U-3000, Thermo, USA) with a UV detector and a Wondasil C18 column (5 mm, 200 × 4.6 mm). The mobile phase consisted of chromatographic methanol and 0.1% phosphoric acid water at a ratio of 65:35 (v/v). The UV visible detector and the operating temperature were set to 228 nm and 35 °C, respectively. The flow rate was 1.0 mL/min and the injection volume was 20 μL. The sample was taken from the middle of the receptor compartment and immediately replenished with an equal volume of the fresh receptor phase (37 °C PBS) after each sample collection. The cumulative amount of IMC released was calculated using the following formula:

$$\text{Cumulative release(\%)} = \frac{C_n \times 6.5 \text{ mL} + \sum_{n=0}^{n-1} C_{n-1} \times 0.5 \text{ mL}}{\text{Initial amount of IMC in the donor compartment}}$$

where C_n and C_{n-1} represented the concentration of IMC in the release medium measured at the n^{th} and $n-1^{\text{th}}$ sample removed, respectively.

2.4.5 X-Ray diffraction (XRD)

The XRD patterns of pure IMC, lyophilized blank KTTKS-Es, physical mixture, and freeze-dried IMC-KTTKS-Es samples were obtained using a D8 Advance X-ray diffractometer (Bruker, Karlsruhe, Germany). The measured voltage and current were 40 kV and 40 mA at ambient temperature respectively, and the X-ray source was Cu K α radiation. Diffraction patterns were collected at 10–80° with 2 θ .

2.4.6. Fourier transform infrared spectroscopy (FTIR)

Fourier transform-infrared (FTIR) spectra of the pure IMC, lyophilized blank KTTKS-Es, physical mixture, and freeze-dried IMC-KTTKS-Es samples were recorded using a Nicolet 6700 Fourier transform infrared spectrophotometer (Thermo Fisher Scientific, USA). The FTIR spectra of samples were scanned over a wavenumber ranging from 400 to 4000 cm⁻¹.

2.5. In vitro percutaneous permeation study

2.5.1. Preparation of skin samples

Porcine ears were obtained from the local slaughterhouse, and domestic pigs were inspected by the quarantine

department. After slaughtering, the porcine ears were cut off immediately, cleaned with tap water and dried immediately with an electric hair dryer, and then the ears were cut into strips of about 3 cm × 3 cm. The porcine ear strips with intact skin were selected, and the skin with a thickness of about 600 μm was obtained with a skin graft knife (Z10100, Shanghai Medical Instrument Co., Ltd.).

2.5.2. Permeation/retention studies in porcine skin

For skin permeation/retention studies, Franz diffusion cells equipment was used. The porcine skin was sandwiched between the donor and acceptor compartment of the vertical diffusion cell with an effective diffusion area of 2.8 cm² and a cell volume of 6.5 mL. A circulating water bath was used to keep the diffusion cells at 37 °C and the receptor medium (pH 7.4 PBS) in the receptor compartment was magnetic stirred continuously at a rate of 300 rpm. 0.5 g of IMC plain gel, IMC-Es gel or IMC-KTTKS-Es gel was gently added to skins, respectively. The experiment was carried out while keeping sink conditions. At the time points of 1, 2, 4, 8, 10, 12, 24 and 48 h, 0.5 mL of the receptor medium in the receptor compartments were withdrawn and replaced immediately with a fresh receptor medium immediately. The samples were assayed by HPLC according to the method described in Section Fourier transform infrared spectroscopy (FTIR). The cumulative amounts of IMC permeated through porcine skins per unit area were plotted as a function of time. The linear regression of the cumulative amount of IMC permeated per unit area (μg/cm²) against time was plotted to determine the drug steady-state permeation rate (*J*_{ss}), which was calculated from the slope of the regression line.

At the end of the skin permeation experiments, the skin was removed and rinsed with deionized water to remove the excess formulation from each skin. Then, the nine full-thickness skins were respectively immersed in 2 mL methanol for 24 h and then kept in an ultrasound bath (KQ-250DE, Kunshan, China) for 0.5 h for the extraction of IMC from the skin. Subsequently, the separation was carried out by refrigerated centrifugation at a speed of 10,000 rpm for 10 min. The amount of skin retention, that is, the total amount of IMC extracted from the skin at the end of the permeation experiments (at 48 h), could be obtained by measuring the content of IMC in the supernatant. The extracted IMC from skins was determined by HPLC.

2.6. Hematoxylin–eosin staining

Hematoxylin and eosin (HE) staining methods were used to study the effect of the formulation on skin microstructure. The skin samples of porcine ears were prepared according to the method described in Section Preparation of skin samples. 0.5 g of physiological saline, IMC plain gel, IMC-Es gel or IMC-KTTKS-Es gel was respectively applied to the donor compartment of the Franz diffusion cells (as per “Permeation/retention studies in porcine skin” section) for 12 h. The skin samples were harvested, rinsed with physiological saline and processed by 4% paraformaldehyde fixation and paraffin

embedding (LEICA EG1160, Nussloch, Germany). Subsequently, samples were cut into longitudinal sections using a slicer (LEICA RM2235, Nussloch, Germany), stained with HE, sealed with neutral gum, and observed for histology analysis using a microscope, respectively.

2.7. Confocal laser scanning microscopy (CLSM) study

Two types of formulation (conventional Es gel and optimized KTTKS-Es gel) loaded with coumarin-6 fluorescent dye were used for the comparative study. Each coumarin 6-loaded formulation was individually studied in vitro on a Franze diffusometer (RYJ-6B, Shanghai, China) protected from light. The skin samples were taken off from the experimental setup after diffusing for 2 h and 12 h, and then rinsed thoroughly with physiological saline to remove any sample deposit. Subsequently, the treated skin samples were cut vertically into 10 μm sections using a freezing slicer (Leica CM1950, Germany) and mounted on a sliding glass with the help of transparent adhesive. The skin sections were dyed by DAPI (1 mg/mL) at 37 °C for 1 min and washed with PBS buffer. The fluorescence in the skin samples was observed by a Confocal microscope (coumarin-6 Ex/Em = 488/519 nm, Leica TCS SPE, Germany).

2.8. In vivo hot plate test in mice

The in vivo analgesic activity was evaluated in mice using the hot plate method (Abdallah et al., 2021). The female mice were placed in the glass cylinder of the intelligent hot plate apparatus (YLS-6B, Jinan, China). The glass cylinder was placed on a heated metal plate with the temperature maintained at about 55.0 °C. The time was recorded immediately after the mice were placed on the hot plate, and the timing was stopped immediately when the first hind paw licking reaction occurred. The mice were divided into four groups, each group containing ten mice. Hot-plate latencies were determined at 30, 60 and 90 min after topical transdermal administration of IMC plain gel, IMC-Es gel or IMC-KTTKS-Es gel at doses of 60.0 mg/kg, blank gel was used as the control group.

2.9. Dimethyl Benzene – induced mice ear edema test

The anti-inflammatory activity of developed formulations was investigated in the acute inflammation method (Gao et al., 2020; Niu et al., 2020). Dimethylbenzene (20 μL per side) was topically applied to both sides of the right ear after 60 min of transdermal administration with the formulation. The left ear remained untreated. The mice were sacrificed by cervical dislocation after being treated with dimethyl benzene for 30 min. The right ear and left ear were cut off at the same position with a stainless steel punch with a diameter of 8 mm and weighed. The ear edema and the inhibitory ratio of ear edema were calculated by the following equation: Ear edema = weight of the right (treated) ear – weight of the left (untreated) ear Inhibitory ratio of ear edema = [(mean of

Table 1. Optimization of the IMC-KTTKS-Es formulation.

Amount of Pal-KTTKS (mg)	Particle size (nm)	PDI	Zeta potential (mV)	EE (%)
0	185.62 ± 9.05	0.138 ± 0.01	−0.28 ± 0.06	65.58 ± 2.32
5	190.57 ± 6.43	0.088 ± 0.01	−37.2 ± 8.52	76.10 ± 1.92
10	195.83 ± 8.80	0.183 ± 0.02	−41.0 ± 8.87	82.42 ± 3.77
20	244.81 ± 9.52	0.225 ± 0.01	−36.4 ± 7.34	82.16 ± 2.94
40	343.39 ± 7.26	0.439 ± 0.03	−30.2 ± 7.66	66.10 ± 1.68

normal control edema – mean of treatment group edema)/mean of normal control edema] × 100%.

2.10. Skin irritation studies

The female mice were engaged to evaluate the skin irritation potential of the formulation. 24 h before the start of the test, hair from the dorsal area (about 2 cm × 2 cm) of mice was carefully removed with an electric shaver and divided into four groups ($n=6$). Further, 0.5 g of the formulation was applied uniformly on the shaved skin of mice, respectively. At 4 h after administration, the residual sample was removed with physiological saline, erythema and/or edema were monitored at the application site for 72 h.

2.11. Statistical analysis

All studies were repeated at least three times. Data were expressed as means ± standard deviation. A Student's *t*-test was used to compare differences between treated groups and control groups. $P < .05$ was considered to be different significantly.

3. Results and discussion

3.1. Optimization of the IMC-KTTKS-Es formulation

Table 1 had shown the changes in these properties with the amount of Pal-KTTKS added to the formulation. When the amount of Pal-KTTKS increased to more than 20 mg, the particle size of IMC-KTTKS-Es suddenly increased from 244.8 nm to more than 343.3 nm, and the particle size distribution range was very wide. The EE of different formulations also showed that the amount over 20 mg of Pal-KTTKS might lead to the instability of the system, resulting in a rapid reduction of the amount of IMC encapsulated in the IMC-KTTKS-Es. Therefore, the optimal amount of Pal-KTTKS in IMC-KTTKS-Es formulation was 20 mg.

3.2. Characterization of IMC-KTTKS-Es

3.2.1. Particle size and zeta potential

In the formulation of a transdermal drug delivery system, particle size is an important constraint. The particle size distribution was uniform (Figure 2A) and the average size of IMC-KTTKS-Es was around 244 nm (Table 1), which was considered to be the appropriate particle size for the transdermal delivery (Danaei et al., 2018). It was previously reported that only particles between 50 and 500 nm in size were possible to penetrate into the skin (Wang et al., 2019). Moreover, previous studies have also shown that

nanoparticles with a diameter of 300 nm or less could transport drugs to the deep layers of the skin to a certain extent, and smaller particle sizes might facilitate drug penetration and deposition in the epidermis and living dermis (Verma et al., 2003; Hua, 2015). The PDI of the optimal IMC-KTTKS-Es dispersions was 0.225 (Table 1). The obtained PDI value was considered to be acceptable for lipid-based carrier drug delivery systems (Chen et al., 2011) and indicated the uniformity of the particle size and low aggregation affinity in the prepared formulation.

The results of zeta potential for the optimal IMC-KTTKS-Es was −36.4 mV (Table 1), which confirmed that the surface charges of the customized formulation were negatively charged. The larger negative potential value of the optimized formulation was due to the change of the net negative surface charge in the presence of KTTKS. Therefore, the formulation was suggested to exhibit a high degree of stability, because previously reported that nanoparticles with absolute zeta potential values greater than 25 mV generally have a high degree of stability (Nasr et al., 2020). The negative charge of the optimized formulation might affect the penetration of IMC through porcine ear skin due to the electrostatic repulsion between the negative charges on the skin surface and the optimized formulation (Malakar et al., 2012). According to previous studies, the negatively charged nanoparticles had improved skin deposition of drugs in transdermal drug delivery (Sinico et al., 2005). The characterization of particle size and zeta potential showed that it was suitable for percutaneous penetration.

3.2.2. Surface morphology

The SEM images clearly delineated that the IMC-KTTKS-Es had a relatively uniform spherical morphology without aggregation (Figure 2B). Moreover, according to the bars in the images, the IMC-KTTKS-Es appeared in particle size of approximately 200 nm. The particle size obtained by SEM was slightly lesser than the result measured by dynamic light scattering (which gives hydrodynamic diameter), which might be due to the dry state of the sample when the scanning electron microscope image was taken.

3.2.3. Encapsulation efficiency (EE)

The EE of optimal IMC-KTTKS-Es measured by the ultrafiltration centrifugation method was 82.16%, which was relatively high. The results proved that the prepared formulation could encapsulate a large dose of IMC, and the IMC-loaded formulation was expected to improve the local therapeutic effect effects (Cai et al., 2021).

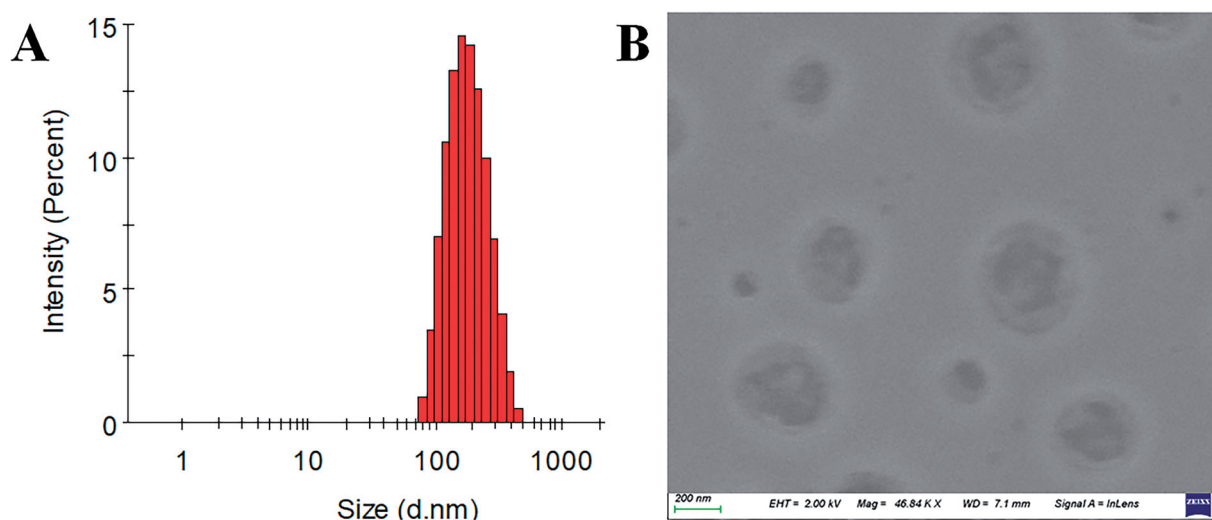


Figure 2. Characterization of formulations. (A) Particle size and distribution of IMC-KTTKS-Es measured by the instrument of Zetasizer Nano; (B) SEM image of IMC-KTTKS-Es.

3.2.4. Deformability measurement

The deformability of the optimized IMC-KTTKS-Es was compared with the IMC-Es and IMC liposomes. Calculations were made using the deformability equation. The deformability values of IMC liposomes, IMC-Es and optimized IMC-KTTKS-Es were 3.59 ± 0.25 , 12.34 ± 0.62 and 11.73 ± 0.46 , respectively. These values indicated that the prepared ethosomes had higher deformability, which was due to the propylene glycol used in the formulation compared with IMC liposomes.

3.2.5. In vitro release

The release profile of IMC from different preparations as a function of time as shown in Figure 3. The IMC plain gel exhibited a rapid release of 57.89% within 48 h, while IMC-Es gel and IMC-KTTKS-Es gel showed a controlled release of 40–44% in 48 h, and the release was slower. This confirmed the interaction between the IMC and the carrier materials in the nanoparticles, resulting in a decrease in the drug release rate and amount. When comparing the release behavior of IMC-Es gel and IMC-KTTKS-Es gel, the release rates of the two samples were similar in the initial 2 h, but after 2 h, the release rate of IMC-KTTKS-Es gel was slightly lower than that of IMC-Es gel. The lower drug release in the IMC-KTTKS-Es gel might be due to the fact that the surface modification of the KTTKS changed the barrier properties of the aqueous boundary layer and the permeability of the membrane. The slow release behavior of the drugs in ethosomes indicated that the phospholipid membrane hinders the diffusion of fat-soluble IMC molecules into the release medium to a certain extent. This could help the drug enter the skin through nanoparticles during topical administration, instead of being released in the form of drug molecules, and then be trapped outside the stratum corneum before the ethosome vesicles penetrate into the skin (Carita et al., 2018).

3.2.6 X-Ray diffraction (XRD)

XRD analysis was used to detect the existence of the crystalline phase, which was also expected to provide indirect evidence for the effective embedding of IMC into KTTKS-Es. The XRD

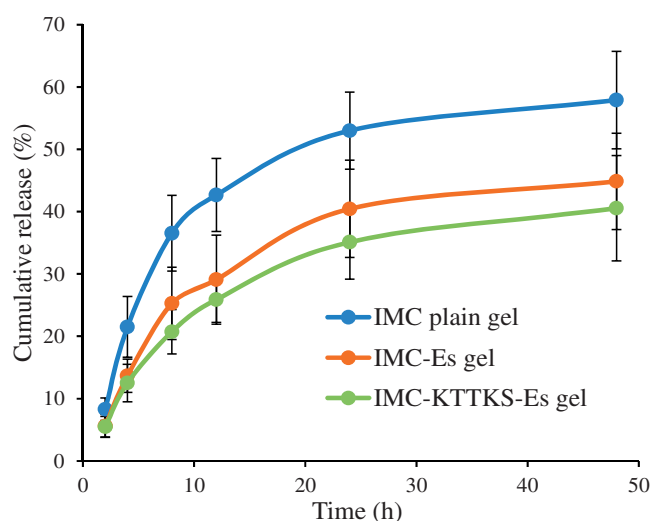


Figure 3. The in vitro release of IMC from IMC plain gel, IMC-Es gel and IMC-KTTKS-Es gel in PBS of pH 7.4.

patterns of IMC, lyophilized blank KTTKS-Es, physical mixture, and freeze-dried IMC-KTTKS-Es were shown in Figure 4(A). No diffraction peak indicated that blank KTTKS-Es were amorphous single phase. The diffraction pattern of IMC showed strong characteristic diffraction peaks of the polymorph, which indicated that the drug was a highly crystalline powder (Zhang et al., 2017). However, after being embedded in KTTKS-Es, no crystalline IMC was detected in the XRD pattern of IMC-KTTKS-Es, indicating that IMC was present in the KTTKS-Es carrier in an amorphous state. It was speculated that when the IMC was loaded into the narrow pores and mesoscale channel of KTTKS-Es, the crystallization of IMC was prevented due to the space confinement, which caused the IMC to become a disordered amorphous state (Zhang et al., 2018).

3.2.7. Fourier transform infrared spectroscopy (FTIR)

Figure 4(B) showed the FTIR spectra of pure IMC, lyophilized blank KTTKS-Es, physical mixture, and freeze-dried IMC-KTTKS-Es. Generally, the C=O stretching vibration peak could be

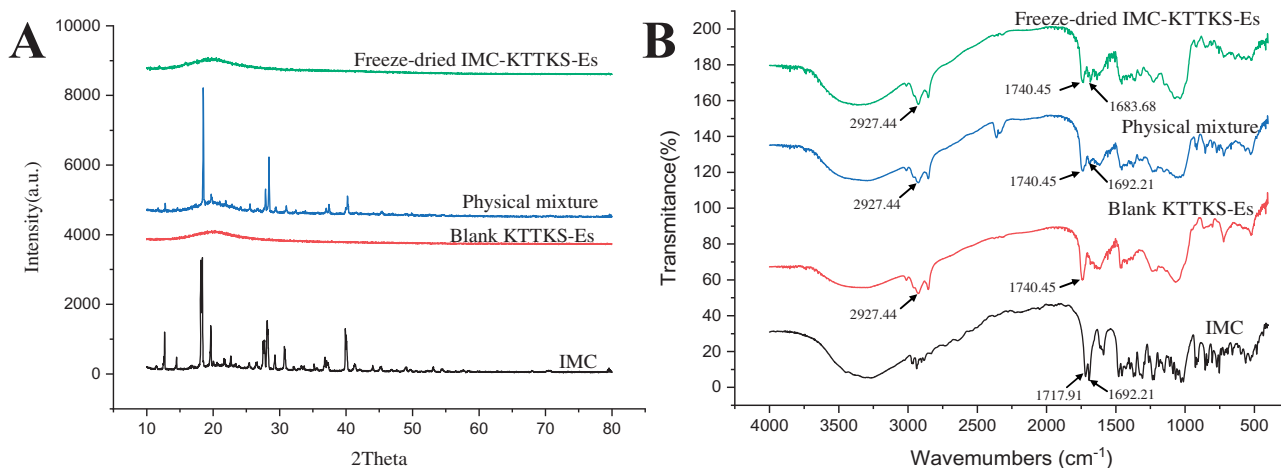


Figure 4. X-ray diffraction patterns (A) and FTIR pattern (B) of pure IMC, lyophilized blank KTTKS-Es, physical mixture, and freeze-dried IMC-KTTKS-Es.

observed in the range of $1600\text{--}1750\text{ cm}^{-1}$. IMC molecule contains two carbonyl groups of benzoyl group and carboxyl group. The peak at 1692.21 cm^{-1} was assigned to benzoyl vibration, while the peak at 1717.91 cm^{-1} might be attributed to the C=O stretching vibration of carboxyl moieties (Zhang et al., 2018). The characteristic peaks of blank KTTKS-Es appeared at 2927.44 cm^{-1} ($-\text{CH}_2-$ stretching vibration peak of $-\text{CH}_2-$ in phospholipids) and 1740.45 cm^{-1} (stretching vibration peak of symmetric C=O in phospholipids), respectively. In the physical mixture system, the vibration peak of benzoyl in the IMC molecules could still be observed at 1692.21 cm^{-1} . However, after incorporation into IMC-KTTKS-Es, the spectra displayed a marked decrease in carbonyl stretching peaks. In addition, a slight shift to the lower wavenumbers occurred, the vibration peak of benzoyl in the IMC molecules shifted from 1692.21 cm^{-1} to 1683.68 cm^{-1} . These results indicated that IMC became amorphous after being encapsulated into the ethosomes, and IMC molecules interact with the carrier materials through hydrogen bonding to form a eutectic mixture. These results were consistent with those reported in the previous literature (Li et al., 2016).

3.3. In vitro skin permeation and retention

The in vitro cumulative permeability of IMC released from IMC plain gel, IMC-Es gel, and IMC-KTTKS-Es gel were evaluated through isolated porcine ear skins. Figure 5(A) showed the cumulative amount of IMC permeated through the unit area of porcine ear skin from three different preparations. As shown in Figure 5(A), the transdermal flux of the IMC in the receptor compartments increased with time, and the graphs showed similar skin penetration patterns for the three different formulations. Obviously, no lag phase was found in any of the ethosome groups, and IMC was detected in the receptor compartment after the first 1 h, indicating that the drugs in the ethosomes could quickly penetrate through the skin. While only a small amount of drugs could be detected in the receptor compartment at 2 h for the preparation of IMC plain gel. The amount of IMC penetrated through the skin for all tested preparations was relatively low within the first 4 h, but the penetration of IMC was significantly ($P < .05$) higher for

IMC-Es gel ($120.08 \pm 15.97\text{ }\mu\text{g}/\text{cm}^2$) and IMC-KTTKS-Es gel ($96.35 \pm 11.03\text{ }\mu\text{g}/\text{cm}^2$) after 48 h compared with that of IMC plain gel ($54.49 \pm 5.25\text{ }\mu\text{g}/\text{cm}^2$).

By encapsulating IMC into ethosomes, the intradermal retention of drugs was highly increased after topical administration (Figure 5B). The current study showed that the skin retention of IMC in IMC-Es gel and IMC-KTTKS-Es gel was higher than that of IMC plain gel. After 48 h of topical administration, the skin retention of IMC in the IMC-Es gel and IMC-KTTKS-Es gel groups was 2.67- and 4.51-fold higher than that in the IMC plain gel group, respectively, and the IMC-KTTKS-Es gel group showed the highest drug retention ($p < .05$). The amount of drug retention in skin tissue for the IMC-KTTKS-Es gel group reached $39.13 \pm 11.58\text{ }\mu\text{g}/\text{cm}^2$. The increased skin retention of IMC-KTTKS-Es gel for topical delivery could be associated with (i) when the particle size of the vesicle was less than 300 nm, it was easy to penetrate the stratum corneum into the skin epidermis and its bottom, and retained in the skin to form a drug reservoir to exert a slow-release effect and achieved the purpose of better treatment of local skin diseases (Verma et al., 2003; Faisal et al., 2018). (ii) negative vesicles might increase the retention of encapsulated lipophilic molecules in the skin, and the improvement of drug retention in negative vesicles might be related to the ability of these vesicles to promote structural changes in the deep layer of the skin, facilitating drug retention into the skin (Ogiso et al., 2001; Maione-Silva et al., 2019). (iii) as a signal peptide in skin tissue, KTTKS could be recognized and bound by signal recognition particles (SRP) in skin tissues, resulting in the retention of KTTKS modified ethosomes in the skin (Tang et al., 2013; Park et al., 2017). In conclusion, IMC-KTTKS-Es gel could increase the intradermal retention of drugs and reduce the number of drugs entering the systemic circulation, and these characteristics are expected to increase the curative effect and reduce the risk of increasing systemic toxicity when used in the treatment of local skin diseases.

3.4. Effect of the preparations on the microstructure of skin

The results of HE staining were shown in Figure 6. The squamous epithelium of porcine skin of the saline group was

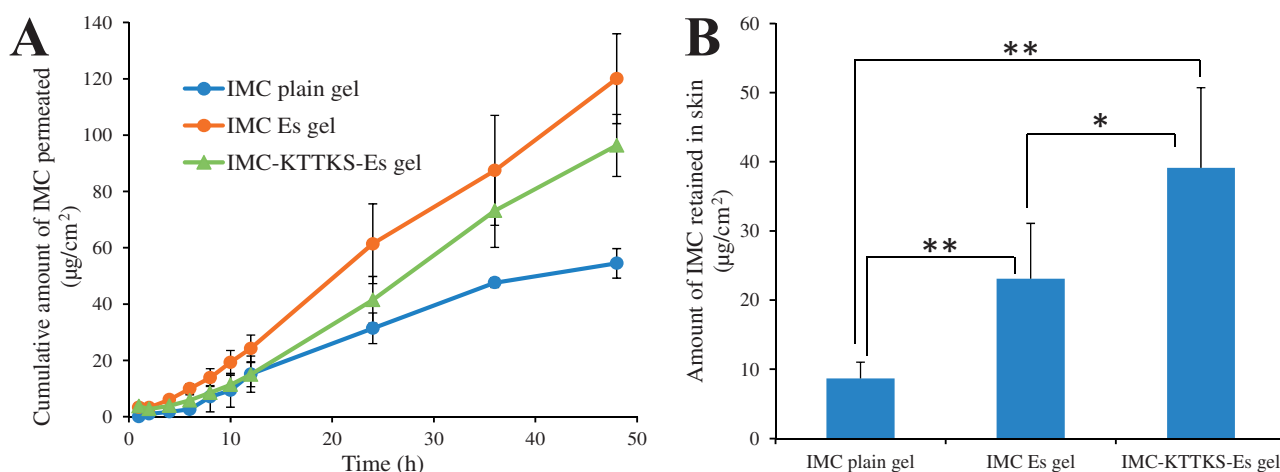


Figure 5. (A) In vitro transdermal delivery of IMC plain gel, IMC-Es gel, and IMC-KTTKS-Es gel in porcine ear skin after 48 h of topical administration. (A) Cumulative transdermal permeation. (B) IMC retention in the skin (data given as the mean \pm SD, $n = 3$; * $p < .05$, ** $p < .01$).

intact and smooth, it was covered with an intact stratum corneum, which was closely associated with the epidermis; the collagen fiber bundles were closely arranged. The skin structure changed after being treated with IMC plain gel, the cuticle structure became loose and thin with slight shedding. However, the phenomena consequential to interactions with the stratum corneum were further intensified after treatment with IMC-Es gel and IMC-KTTKS-Es gel, and the stratum corneum layer became looser and thin with distinctly shedding, as compared with the IMC plain gel group. The stratum corneum was an important barrier to protect the skin from foreign substances, and its structure is disturbed by ethosome nanovesicles, which was conducive to drug entry or delivery through the skin. Furthermore, the outstanding deformation ability of ethosome could make it penetrate into the intercellular space of the outermost layer of stratum corneum and into the deep layer of stratum corneum, which might further promote its fusion with the lipid components of keratinocytes and change the structure of stratum corneum more effectively than rigid liposomal vesicles, which only affect the surface of stratum corneum in an incremental manner (Zhang et al., 2015).

3.5. Confocal laser scanning microscopy (CLSM) studies

The CLSM images of the longitudinal sections of porcine ear skin obtained 1 h and 12 h after the application of COU-Es gel and COU-KTTKS-Es gel was shown in Figure 7. It could be seen from Figure 7 that after 1 h of administration, the COU-KTTKS-Es gel group and COU-Es gel group showed strong fluorescence in both the epidermis and dermis, indicating that the preparation of ethosome could overcome the SC barrier and promote the penetration of drugs. The fluorescence of skin treated with COU-Es gel decreased after 12 h, most of the coumarin-6 fluorescence remains in the skin appendages, while intense fluorescence was observed in the deep skin and skin appendages beneath the epidermis in the COU-KTTKS-Es gel group and the fluorescence intensity of deep skin in COU-KTTKS-Es gel group was higher than that in COU-Es gel group at 12 h. These results indicated that

KTTKS modified ethosomes had better targeting of local skin tissues than conventional ethosomes, thereby effectively ensuring the treatment of topical skin diseases that require transdermal delivery.

3.6. Assessment of analgesic activity

According to Table 2, the tested medicated formulations had a significant topical analgesic effect, while the control group was reported to be no significant increase in reaction time within an overall 90 min of treatment. The longest response times of IMC-Es gel and IMC-KTTKS-Es gel treated for 90 min were 26.50 s and 35.55 s, respectively, while the longest response times of the negative control group and IMC plain gel were 16.79 s and 19.41 s, respectively. It is obvious that the transdermal administration of IMC-Es gel and IMC-KTTKS-Es gel showed a significantly prolonged time of mice responses toward the thermal pain at all time intervals, compared with the negative control group and IMC plain gel group ($P < .05$). The high deformability of IMC-ethosomal nanoparticles might be the main reason for the better analgesic performance of IMC-ethosomes compared to its plain formulation. Compared with the IMC-Es gel treatment group, the IMC-KTTKS-Es gel treatment group showed a significantly higher analgesic effect ($p < .05$) at 90 min following topical application of the formulation. The modification of ethosomes by KTTKS might increase the retention of IMC in the skin of mice, thereby achieving higher skin bioavailability and therapeutic analgesic potential.

3.7. Assessment of anti-inflammatory activity

The results showed that the inhibition rate ($52.89 \pm 8.56\%$) of IMC-KTTKS-Es gel significantly increased ($p < .05$) compared with that of IMC plain gel ($31.99 \pm 6.72\%$) and IMC-Es gel ($38.58 \pm 7.48\%$). Based on these results, it could be concluded that the IMC-KTTKS-Es gel was the most effective formulation against dimethyl benzene-induced skin inflammation and damage.

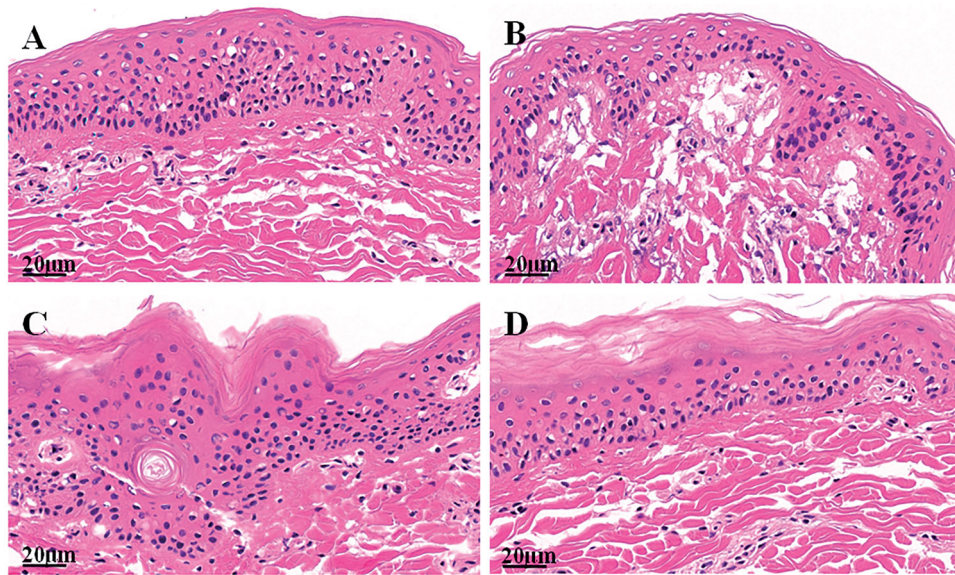


Figure 6. Micrographs of the hematoxylin-eosin (HE) stained porcine ear sections after being treated with (A) Physiological saline (B) IMC plain gel (C) IMC-Es gel and (D) IMC-KTTKS-Es gel.

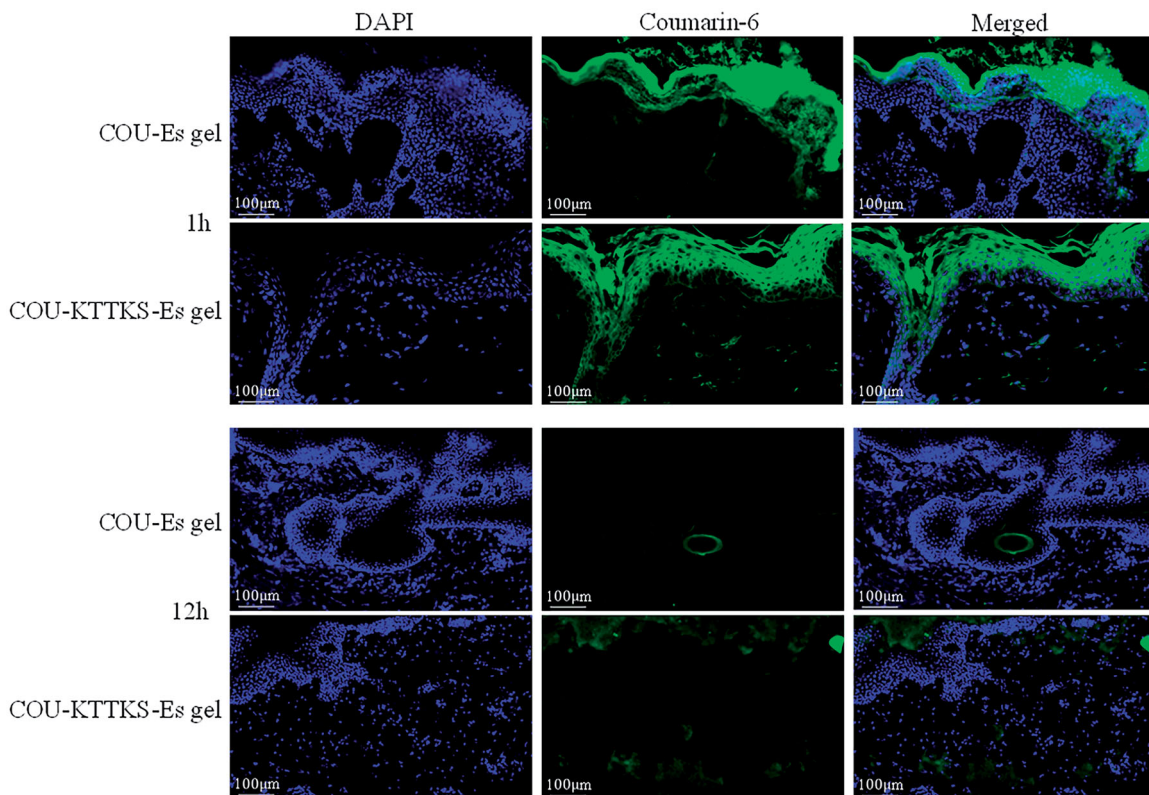


Figure 7. CLSM images of the vertical section of the skin treated with the various formulations post administration. The slides were stained with DAPI.

Table 2. Mean reaction time of control, IMC plain gel, IMC-Es gel and IMC-KTTKS-Es gel in mice at various time intervals.

Formulation	Pre-treatment (s)	Reaction time (s)		
		30 min	60 min	90 min
Control	15.49 ± 3.65	15.39 ± 3.26	15.11 ± 4.72	16.79 ± 7.65
IMC plain gel	14.79 ± 2.45	16.25 ± 3.48	20.91 ± 6.59*	19.41 ± 5.65*
IMC-Es gel	15.58 ± 4.53	22.25 ± 6.14*#	29.21 ± 6.30*#	26.50 ± 8.98*#
IMC-KTTKS-Es gel	14.99 ± 2.89	20.86 ± 4.96*#	31.59 ± 5.89*#	35.55 ± 6.78*# [§]

* $p < .05$ vs. control group, # $p < .05$ vs. IMC plain gel, $^{\S}p < .05$ vs. IMC-Es gel treated group.

3.8. In vivo skin irritation test

Skin irritation studies showed that none of the IMC formulations showed skin irritation. No erythema and edema were observed in the dorsal coastal region (Figure 8). These results indicated that all of the ingredients in the formulation (phospholipids, Pal-KTTKS, propylene glycol, Carbopol 940®) were well tolerated and never sensitized to the skin. Therefore, IMC-KTTKS-Es gel might be a safe and well-tolerated delivery vehicle of IMC for topical application.

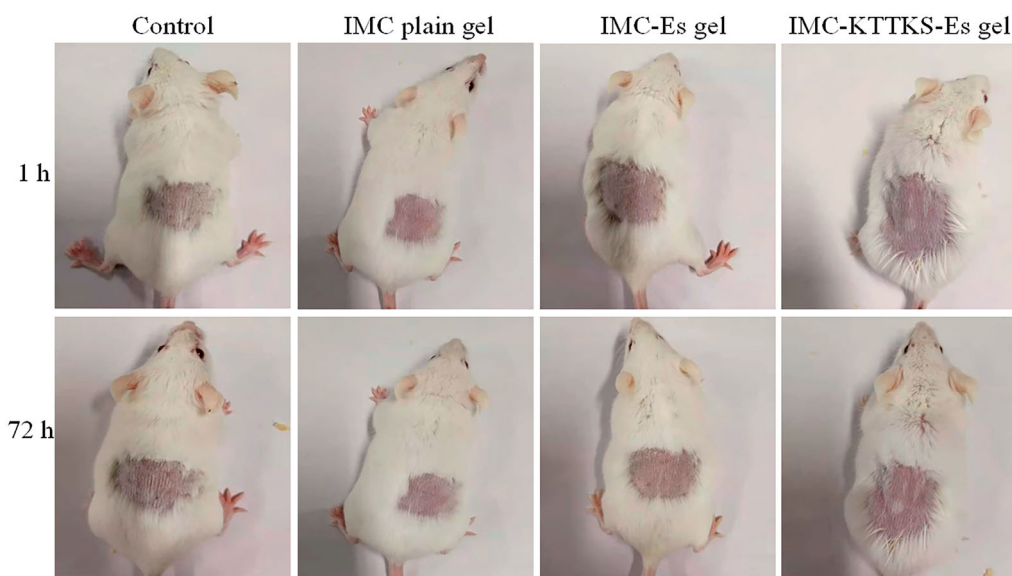


Figure 8. In vivo skin irritation test. Skin appearance of mice observed at 1 and 72 h.

4. Conclusions

In this study, IMC-KTTKS-Es had been successfully prepared by thin-film evaporation and hydration method, fully characterized and evaluated after being loaded with the lipophilic IMC, and its gel was used to transport IMC through the skin to achieve topical analgesia and anti-inflammatory. In vitro skin, transdermal study and CLSM evaluation showed that IMC-KTTKS-Es could enhance the skin retention effect of IMC when topical administration. The enhanced analgesic efficacy of IMC-KTTKS-Es gel was significant ($P < .05$) compared to IMC-Es gel of the same dose. Similarly, the anti-inflammatory activity of IMC-KTTKS-Es gel was stronger than that of IMC-Es gel in dimethyl benzene-induced ear swelling of mice. Furthermore, irritation studies illustrated that the IMC-KTTKS-Es gel did not cause any skin irritation. Overall, these results showed that IMC-KTTKS-Es gel might be a promising transdermal delivery vector for topical analgesia and anti-inflammatory.

Disclosure statement

No potential conflict of interest was reported by the author(s).

Funding

We are grateful for the financial support from the Key Scientific Research Project of Higher Education of Henan Province (No.20B180006), the National project cultivation fund of Luoyang Normal University (No.2019-PYJJ-012) and key scientific and technological project of Henan of China (No.202102110103).

References

Abd E, Gomes J, Sales CC, et al. (2021). Deformable liposomes as enhancer of caffeine penetration through human skin in a Franz diffusion cell test. *Int J Cosmet Sci* 43:1800–10.

Abdallah MH, Abu Lila AS, Unissa R, et al. (2021). Preparation, characterization and evaluation of anti-inflammatory and anti-nociceptive effects of brucine-loaded nanoemulgel. *Colloids Surf B Biointerfaces* 205:111868.

Aragao Horoiwa T, Cortez M, Sauter IP, et al. (2020). Sugar-based colloidal nanocarriers for topical meglumine antimoniate application to cutaneous leishmaniasis treatment: ex vivo cutaneous retention and in vivo evaluation. *Eur J Pharm Sci* 147:105295.

Bae Y, Lee J, Kho C, et al. (2021). Apoptin gene delivery by a PAMAM dendrimer modified with a nuclear localization signal peptide as a gene carrier for brain cancer therapy. *Korean J Physiol Pharmacol* 25: 467–78.

Cai W, Liu J, Zheng L, et al. (2021). Study on the anti-infection ability of vancomycin cationic liposome combined with polylactide fracture internal fixator. *Int J Biol Macromol* 167:834–44.

Carita AC, Eloy JO, Chorilli M, et al. (2018). Recent advances and perspectives in liposomes for cutaneous drug delivery. *Curr Med Chem* 25: 606–35.

Chen M, Liu X, Fahr A. (2011). Skin penetration and deposition of carboxyfluorescein and temoporfin from different lipid vesicular systems: in vitro study with finite and infinite dosage application. *Int J Pharm* 408:223–34.

Danaei M, Dehghankhold M, Ataei S, et al. (2018). Impact of particle size and polydispersity index on the clinical applications of lipidic nanocarrier systems. *Pharmaceutics* 10:57.

Doppalapudi S, Jain A, Chopra DK, et al. (2017). Psoralen loaded liposomal nanocarriers for improved skin penetration and efficacy of topical PUVA in psoriasis. *Eur J Pharm Sci* 96:515–29.

Dudhipala N, Phasha Mohammed R, Adel Ali Youssef A, et al. (2020). Effect of lipid and edge activator concentration on development of aceclofenac-loaded transfersomes gel for transdermal application: in vitro and ex vivo skin permeation. *Drug Dev Ind Pharm* 46: 1334–44.

El Maghraby GM. (2010). Self-microemulsifying and microemulsion systems for transdermal delivery of indomethacin: effect of phase transition. *Colloids Surf B Biointerfaces* 75:595–600.

Faisal W, Soliman GM, Hamdan AM. (2018). Enhanced skin deposition and delivery of voriconazole using ethosomal preparations. *J Liposome Res* 28:14–21.

Froelich A, Osmatek T, Snela A, et al. (2017). Novel microemulsion-based gels for topical delivery of indomethacin: formulation, physicochemical properties and in vitro drug release studies. *J Colloid Interface Sci* 507:323–36.

Gao H, Kang N, Hu C, et al. (2020). Ginsenoside Rb1 exerts anti-inflammatory effects in vitro and in vivo by modulating toll-like receptor 4

- dimerization and NF- κ B/MAPKs signaling pathways. *Phytomedicine* 69:153197.
- Hua S. (2015). Lipid-based nano-delivery systems for skin delivery of drugs and bioactives. *Front Pharmacol* 6:219.
- Kapoor MS, GuhaSarkar S, Banerjee R. (2017). Stratum corneum modulation by chemical enhancers and lipid nanostructures: implications for transdermal drug delivery. *Ther Deliv* 8:701–18.
- Li J, Xu L, Wang H, et al. (2016). Comparison of bare and amino modified mesoporous silica@poly(ethyleneimine)s xerogel as indomethacin carrier: superiority of amino modification. *Mater Sci Eng C Mater Biol Appl* 59:710–6.
- Maione-Silva L, de Castro EG, Nascimento TL, et al. (2019). Ascorbic acid encapsulated into negatively charged liposomes exhibits increased skin permeation, retention and enhances collagen synthesis by fibroblasts. *Sci Rep* 9:522.
- Malakar J, Sen SO, Nayak AK, et al. (2012). Formulation, optimization and evaluation of transferosomal gel for transdermal insulin delivery. *Saudi Pharm J* 20:355–63.
- Nagai N, Ogata F, Yamaguchi M, et al. (2019). Combination with l-menthhol enhances transdermal penetration of indomethacin solid nanoparticles. *Int J Mol Sci* 20:3644.
- Nasr M, Younes H, Abdel-Rashid RS. (2020). Formulation and evaluation of cubosomes containing colchicine for transdermal delivery. *Drug Deliv Transl Res* 10:1302–13.
- Niu J, Yuan M, Chen C, et al. (2020). Berberine-loaded thiolated pluronic F127 polymeric micelles for improving skin permeation and retention. *Int J Nanomedicine* 15:9987–10005.
- Ogiso T, Yamaguchi T, Iwaki M, et al. (2001). Effect of positively and negatively charged liposomes on skin permeation of drugs. *J Drug Target* 9:49–59.
- Park H, An E, Cho Lee AR. (2017). Effect of Palmitoyl-Pentapeptide (Pal-KTTKS) on wound contractile process in relation with connective tissue growth factor and alpha-smooth muscle actin expression. *Tissue Eng Regen Med* 14:73–80.
- Sinico C, Manconi M, Peppi M, et al. (2005). Liposomes as carriers for dermal delivery of tretinoin: in vitro evaluation of drug permeation and vesicle-skin interaction. *J Control Release* 103:123–36.
- Talaaj U, Uscinowicz P, Bruzgo I, et al. (2019). The effects of a novel series of KTTKS analogues on cytotoxicity and proteolytic activity. *Molecules* 24:3698.
- Tang S, Lucius R, Wenck H, et al. (2013). UV-mediated downregulation of the endocytic collagen receptor, Endo180, contributes to accumulation of extracellular collagen fragments in photoaged skin. *J Dermatol Sci* 70:42–8.
- Toropainen E, Fraser-Miller SJ, Novakovic D, et al. (2021). Biopharmaceutics of topical ophthalmic suspensions: importance of viscosity and particle size in ocular absorption of indomethacin. *Pharmaceutics* 13:452.
- Vasanth S, Dubey A, G SR, et al. (2020). Development and investigation of vitamin C-enriched adapalene-loaded transfersome gel: a collegial approach for the treatment of acne vulgaris. *AAPS PharmSciTech* 21: 61.
- Verma DD, Verma S, Blume G, et al. (2003). Particle size of liposomes influences dermal delivery of substances into skin. *Int J Pharm* 258: 141–51.
- Wang WX, Feng SS, Zheng CH. (2016). A comparison between conventional liposome and drug-cyclodextrin complex in liposome system. *Int J Pharm* 513:387–92.
- Wang Y, Wang X, Wang X, et al. (2019). Design and development of lidocaine microemulsions for transdermal delivery. *AAPS PharmSciTech* 20:63.
- Zhang W, Zhang CN, He Y, et al. (2017). Factors affecting the dissolution of indomethacin solid dispersions. *AAPS PharmSciTech* 18:3258–73.
- Zhang W, Zheng N, Chen L, et al. (2018). Effect of shape on mesoporous silica nanoparticles for oral delivery of indomethacin. *Pharmaceutics* 11:4.
- Zhang Y, Shen L, Zhang K, et al. (2015). Enhanced antioxidation via encapsulation of isooctyl p-methoxycinnamate with sodium deoxycholate-mediated liposome endocytosis. *Int J Pharm* 496:392–400.
- Zhang YT, Shen LN, Wu ZH, et al. (2014). Comparison of ethosomes and liposomes for skin delivery of psoralen for psoriasis therapy. *Int J Pharm* 471:449–52.